Proc. Natl. Acad. Sci. USA
Vol. 86, pp. 2693–2697, April 1989
Cell Biology

Generation of fibrosarcomas *in vivo* by a retrovirus that expresses the normal B chain of platelet-derived growth factor and mimics the alternative splice pattern of the v-*sis* oncogene

(selection/tumorigenesis/clonality)

M. PECH, A. GAZIT*, P. ARNSTEIN, AND S. A. AARONSON

Laboratory of Cellular and Molecular Biology, National Cancer Institute, Bethesda, MD 20892

Communicated by Peter Duesberg, January 6, 1989

ABSTRACT **A retrovirus containing the entire human platelet-derived growth factor B-chain (PDGF-B) gene was constructed in order to investigate the *in vivo* biological activity of its encoded growth factor. When this virus was introduced into newborn mice, it reproducibly generated fibrosarcomas at the site of inoculation. Proviruses in each fibrosarcoma analyzed had lost 149 nucleotides downstream of the PDGF-B coding region. This deletion originated from an alternative or aberrant splice event that occurred within exon 7 of the PDGF-B gene and mimicked the v-*sis* oncogene. Thus, deletion of this region may be necessary for efficient retrovirus replication or for more potent transforming function. Evidence that the normal growth factor coding sequence was unaltered derived from RNase protection studies and immunoprecipitation analysis. Tumors were generally polyclonal but demonstrated clonal subpopulations. Moreover, tumor-derived cell lines became monoclonal within a few tissue culture passages and rapidly formed tumors *in vivo*. These findings argue that overexpression of the normal human PDGF-B gene product under retrovirus control can induce the fully malignant phenotype.**

The v-*sis* oncogene of simian sarcoma virus (SSV) encodes a protein, $p28^{v\text{-}sis}$, that is closely related to the human platelet-derived growth factor B chain (PDGF-B) (1, 2). The c-*sis*/PDGF-B gene (*SIS/PDGFB*), the human homologue for v-*sis*, has been cloned and characterized (3). When this gene is expressed under the control of a retroviral promoter and introduced into NIH 3T3 cells in culture, it confers the transformed phenotype on these cells (4). The PDGF-B transcript has been observed in a variety of human glioblastomas and fibrosarcomas (5). In contrast, this transcript is not detectable in normal glial cells or fibroblasts. All of these findings, along with the immunological demonstration of PDGF-B protein expressed by such human tumor cells (6), support a role of PDGF-B in tumorigenesis.

Although the ability of a gene to cause transformation of a continuous cell line in culture argues for its transforming potential, NIH 3T3 cells differ significantly from normal diploid cells. Several approaches including the use of retroviral vectors (7) and transgenic mice (8) have been utilized to assess the ability of a gene to initiate steps leading to malignancy *in vivo*. We decided to construct a retrovirus from the human PDGF-B gene in order to investigate the biologic activities of its encoded growth factor on diploid cells *in vivo*. At the same time, expressing the complete PDGF-B gene within a retrovirus construct provided us the opportunity to study the effects of selection within the retrovirus on the structure and function of this gene.

The publication costs of this article were defrayed in part by page charge payment. This article must therefore be hereby marked "*advertisement*" in accordance with 18 U.S.C. §1734 solely to indicate this fact.

MATERIALS AND METHODS

Cells and Viruses. Continuous mouse NIH 3T3 (9) and SSV-infected producer marmoset (HF/SSV) (10) cell lines have been described. To rescue virus from NIH 3T3 cells transfected with plasmid pPDGF-B, the mouse type C helper virus AP 129 (11) was used.

Transfection Assays. DNA transfection of NIH 3T3 cells was performed by a modified calcium phosphate precipitation technique (12). Plasmid pPDGF-B was mixed with pSV2-neo (13) DNA at a 10:1 molar ratio for transfection, and NIH 3T3 cells expressing the *neo* gene were selected by their ability to grow in the presence of the neomycin analogue G418 at 750 μg/ml.

Plasmid Constructions. Standard protocols were used for all recombinant DNA techniques (14). A subclone (15) of integrated Abelson murine leukemia virus (Ab-MuLV) was used as a retroviral vector. All Ab-MuLV coding sequences between the *Bst*EII (position 1171 in ref. 16) and *Bam*HI (position 4800) restriction sites were deleted and replaced by an *Eco*RI site into which genomic PDGF-B sequences from λ c-*sis* clones 8 (3) and 10 (17) were inserted. The resulting plasmid, pPDGF-B, contains all the PDGF-B coding and flanking sequences between the *Eco*RI sites in the c-*sis* locus (18). DNA and RNA probes were derived from subcloning fragments of pcsis4.0 and pGSS2.7 (19) and of λ c-*sis* clone 10 (17) into pGEM-1 and -4 (Promega). A 540-base-pair (bp) *Sac* I–*Kpn* I fragment of the mouse β_2-microglobulin gene (20) and a human β-actin RNA probe derived from a cDNA clone (21) were employed to standardize DNA amounts.

Virus Inoculation and Tumorigenicity Assays. PDGF-B (AP 129) virus or the AP 129 helper virus alone were inoculated intramuscularly, subcutaneously, and/or intracranially into newborn euthymic NFR mice. Athymic nude NFR (*nu/nu*) mice were used for tumorigenicity assays.

Metabolic Labeling and Immunoprecipitation. Cells metabolically labeled with [^{35}S]methionine and [^{35}S]cysteine were lysed and immunoprecipitation with anti-PDGF and anti-sis-C was performed as described (6).

DNA Blotting Analysis. Proviral copy numbers were determined in serial dilutions of cellular DNAs slot-blotted on a Minifold II apparatus (Schleicher & Schuell) by hybridization to RNA probe V (Fig. 4). Hybridization to β_2-microglobulin or β-actin probes was employed to control for the amounts of DNA. Autoradiograms of slot blots were scanned in a Bio-Rad model 620 video densitometer, and proviral copy numbers were calculated by comparing signal intensities to those generated by various dilutions of DNA from normal diploid fibroblasts and of plasmid pcsis4.0. Southern blot analysis was performed by standard procedures (14).

Abbreviations: PDGF-B, B chain of platelet-derived growth factor; SSV, simian sarcoma virus.

*Present address: Sackler School of Medicine, Tel Aviv University, Tel Aviv 69978, Israel.

RNA Sequencing. Total cellular RNA was used for sequence determination, performed as described by Geliebter *et al.* (22).

RNase Protection Assays. Assays were done according to Melton *et al.* (23) under conditions recommended by the supplier of the SP6 and T7 polymerases (Promega).

RESULTS

Inoculation of Newborn Mice with a Retrovirus Containing the Human PDGF-B Coding Region Causes Tumor Formation. We included the entire PDGF-B gene in our retroviral expression system in order to be able to monitor the appearance of retroviral variants after selection *in vivo*. After transfection of NIH 3T3 cells with pPDGF-B (*Materials and Methods*), PDGF-B virus was rescued by superinfection with the helper virus AP 129 and shown to be capable of inducing the transformed phenotype upon infection of NIH 3T3 cells.

To assess the biological activity of the growth factor-encoding retrovirus *in vivo*, we inoculated newborn NFR mice. Of 24 animals injected with 10^3 focus-forming units, 20 developed tumors at the site of inoculation within 3–7 months. Histological examination revealed each to be a moderately well differentiated fibrosarcoma. Of 14 fibrosarcomas tested for the ability to be passaged *in vivo*, all could be transplanted into NFR *nu/nu* mice. In contrast, inoculation with the AP 129 helper virus alone failed to induce any sarcomas. Thus, the PDGF-B virus induced a very specific tumor phenotype independent of the site of inoculation.

PDGF-B Virus-Induced Fibrosarcomas Express the Normal PDGF-B Polypeptide. To investigate the expression of the PDGF-B protein, we used antisera directed against human PDGF or against the carboxyl-terminal portion of $p28^{v\text{-}sis}$. Analysis of two fibrosarcoma cell lysates by immunoprecipitation revealed different forms of PDGF-B (Fig. 1). These forms were indistinguishable from the known PDGF-B products found in COS-1 cells expressing the normal human PDGF-B cDNA (6).

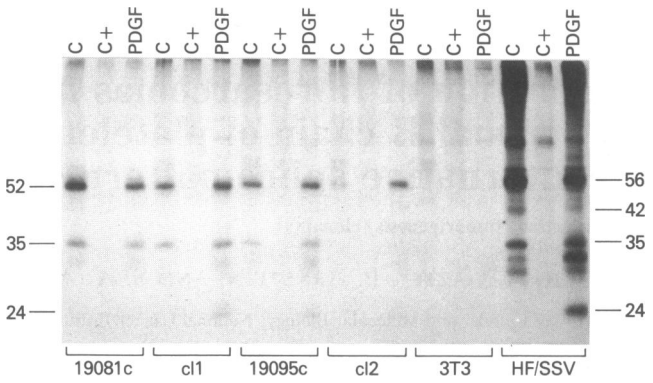

FIG. 1. Expression of normal PDGF-B chain after *in vivo* and *in vitro* transformation by PDGF-B virus. Two PDGF-B virus-induced fibrosarcoma cell lines (19081c and 19095c), two clonal NIH 3T3 cell lines (cl1 and cl2) transformed by PDGF-B virus, uninfected NIH 3T3 cells (3T3), and a SSV-transformed marmoset cell line (HF/SSV) were metabolically labeled. Cell lysates were immunoprecipitated with anti-sis-C (lanes C), anti-sis-C preincubated with homologous peptide (lanes C+), or anti-PDGF (lanes PDGF) and analyzed by $NaDodSO_4$/PAGE. Sizes (kDa) of PDGF-B virus-encoded proteins are given at left and those encoded by SSV are shown at right. The 52-kDa product has been identified as the largest PDGF-B precursor after dimerization and N-linked glycosylation of the 26-kDa primary product (6). The 35-kDa species is generated by N-terminal cleavage followed by C-terminal processing leading to the fully processed p24. $NaDodSO_4$/PAGE under reducing conditions showed predominantly a $p26^{c\text{-}sis}$ monomer (data not shown).

We employed RNase protection assays with various RNA probes to map any alterations between the coding regions in normal PDGF-B mRNA and PDGF-B virus RNA. An example of one such mapping experiment is shown in Fig. 2. The

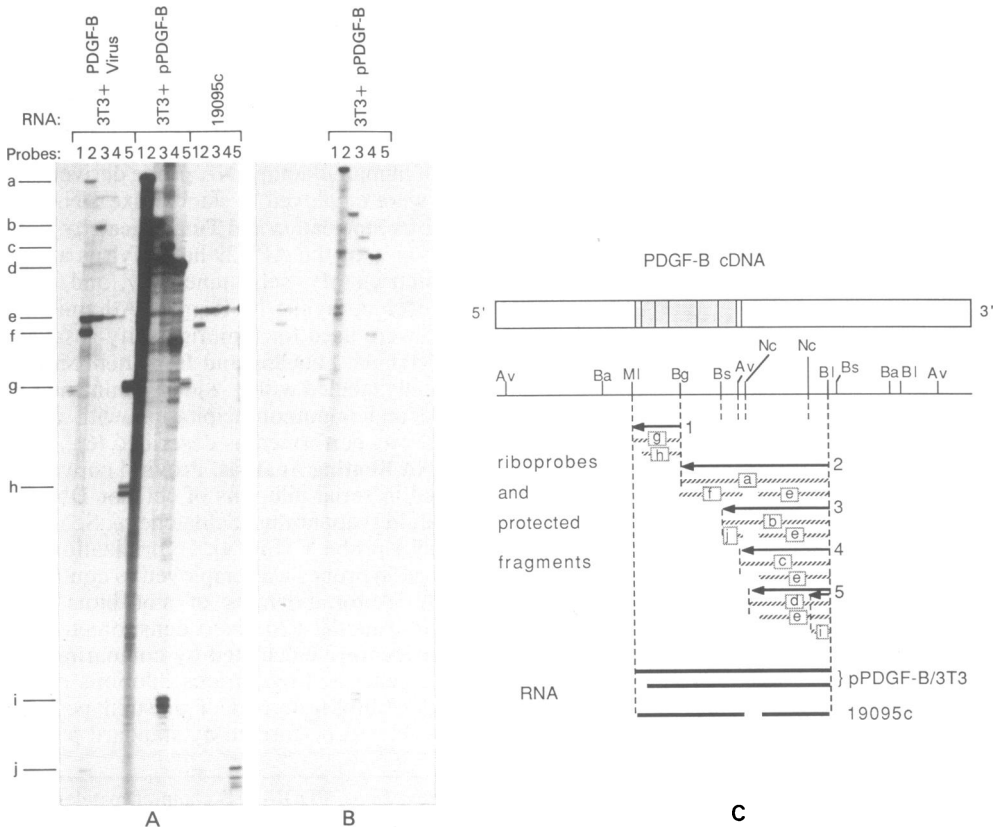

FIG. 2. (*Legend appears at the bottom of the opposite page.*)

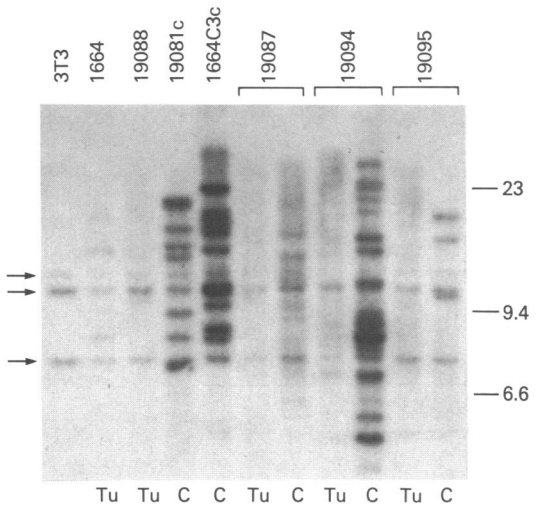

FIG. 3. Hybridization pattern of integrated PDGF-B provirus in fibrosarcomas before and after passage in cell culture. High molecular weight DNAs were isolated from primary fibrosarcomas (lanes Tu) and fibrosarcoma-derived cell lines (lanes C). The DNAs were digested with *Hin*dIII, which does not cut within PDGF-B cDNA or viral vector sequences, and hybridized with a radioactively labeled *Mlu* I–*Avr* II fragment from PDGF-B cDNA. Thus, each band represents a different proviral integration site. DNAs from 19095, 19094, and 19087 were prepared from tumor tissues (Tu) or from cells (C) originating from these tissues after 1 (19087c) or 11 (19094c and 19095c) passages in culture. Arrows indicate bands that represent the endogenous mouse PDGF-B gene; its hybridization pattern was used as an internal control. Positions of *Hin*dIII fragments of phage λ DNA are shown as a size reference (lengths given in kilobases).

PDGF-B coding region of RNA from the PDGF-B virus-induced fibrosarcoma 19095c was fully protected by an RNA probe derived from PDGF-B cDNA. By using this approach, it was possible to show that the coding region of PDGF-B virus RNA in seven independent fibrosarcomas and five fibrosarcoma cell lines was indistinguishable from normal PDGF-B RNA. Thus, our results indicated that the viral PDGF-B coding region was unaltered by even minor genetic changes that could have contributed to the transforming properties of the human PDGF-B protein.

Proviral Integration Patterns in PDGF-B Virus-Induced Mouse Fibrosarcomas. Tumors induced by the PDGF-B virus could originate from an expanding polyclonal population of growth-stimulated cells or from single malignant cells. Since retroviral DNA is known to integrate into many different sites within the cellular genome (7), the detection of identically integrated copies within the tumor DNA would argue for the presence of a clonal population. To address this question, DNAs of several PDGF-B virus-induced fibrosarcomas were subjected to Southern blot analysis using PDGF-B cDNA as a probe. As shown in Fig. 3, one tumor DNA (no. 1664) showed only distinct bands, implying a clonal or oligoclonal cell population. The other tumor DNAs displayed a generalized increased intensity of hybridization, indicating a polyclonal population. However, the detection of fragments superimposed on this background implied the presence of a minor population of clonally derived cells.

Table 1. Copy numbers and integration sites of the PDGF-B provirus

Source*	No. of sites†	Copy number‡	Clonality
Primary tumors			
19095	TMC	NT	Polyclonal with clonal subpopulations
19094	TMC	15	
19087	TMC	13	
19088	TMC	2	
19074	TMC	6	
1664-1	TMC	6	
1664	3	0.5	Mono/oligoclonal
Tumor cell lines			
19095c	4	5	Mono/oligoclonal
19094c	19	NT	
19081c	8	8	
19087c	>14	NT	
1664C3c	13	18	
Transformed cells			
3T3-cl1	5	5	Monoclonal
3T3-cl2	3	3	
3T3-cl3	2	2	

*Tumors and cell lines (c) derived from them are identified by identical numbers. NIH 3T3 cells transformed by PDGF-B virus (3T3-cl1–3) were cloned in soft agar.
†Estimated from the number of *Hin*dIII fragments (Fig. 3) in digests of cellular DNAs hybridizing with probe III (Fig. 4). TMC, too many to count (continuous hybridization signal with superimposed weak bands).
‡Calculated from signal intensities in slot blots of serially diluted cellular DNAs (*Materials and Methods*). NT, not tested.

In those cases where cell lines were established from the fibrosarcomas, there was a rapid selection for clonal or oligoclonal cell populations within 1–11 passages in cell culture (Fig. 3, lanes C). Such cultured tumor cells were rapidly tumorigenic and formed large (30 × 30 mm) fibrosarcomas within 20–30 days after inoculation of 10^6 cells into nude mice. Thus, clonal selection of PDGF-B virus-transformed cells led to a fully neoplastic population.

The large number of differently integrated proviruses in some tumor cell lines raised the question as to whether the cell population was monoclonal with more than one proviral copy or was composed of as many as 13–19 different clones with each containing a single provirus (Fig. 3, cell lines 19094c and 1664C3c). By quantitative slot blot analysis, it was shown that the average number of proviral copies per genome corresponded closely in each case to the number of integrated proviruses detected by Southern blot analysis in the same tumor cell line (Table 1). Thus, the tumor cell lines contain a predominantly clonal population, in each case with multiple integrated proviral copies.

PDGF-B Viruses in Fibrosarcomas Have Suffered a Deletion Outside of the PDGF-B Coding Region. To further determine

FIG. 2 (*on opposite page*). RNase protection mapping of PDGF-B RNAs. RNase protection assays were performed with total cellular RNAs isolated from the NIH 3T3 cell mass population transfected with pPDGF-B (3T3 + pPDGF-B), from a fibrosarcoma induced by inoculation with the PDGF-B virus stock (19095c), and from NIH 3T3 cells infected with PDGF-B virus that had been passaged once in NIH 3T3 cells (3T3 + PDGF-B virus). The RNAs were first hybridized to five different antisense RNA probes (*A–C*, riboprobes 1–5) derived from PDGF-B cDNA (stippled boxes: coding region), and then treated with RNase. *A* and *B* show different exposures of an autoradiogram of a 5% polyacrylamide sequencing gel where the protected fragments (a–j) were separated. The extent and localization of the protected fragments in *A* and *B* are symbolized in *C* by hatched bars. Deletions are indicated by gaps. pPDGF-B-transfected NIH 3T3 cells contain two major RNA species, symbolized by heavy lines near the bottom of *C*. Normal, correctly spliced PDGF-B RNA is characterized by protected fragments a–d and g (*A–C*). Fragment h in pPDGF-B-transfected NIH 3T3 cells is due to an RNA species missing exon 1 sequences. The fibrosarcoma line 19095c contains only one type of PDGF-B RNA (interrupted heavy line in *C*), which has the complete PDGF-B coding sequence. The presence of a 149-nucleotide deletion outside of the PDGF-B coding region results in fragments e and f (*A–C*) being protected against RNase digestion. PDGF-B virus-infected NIH 3T3 cells contain PDGF-B RNA with and without the 149-nucleotide deletion. Riboprobe 5 consists of two RNA species. Restriction endonuclease sites: Av, *Avr* II; Ba, *Bam*HI; Bg, *Bgl* II; Bl, *Bal* I; Bs, *Bst*EII; Ml, *Mlu* I; Nc, *Nco* I.

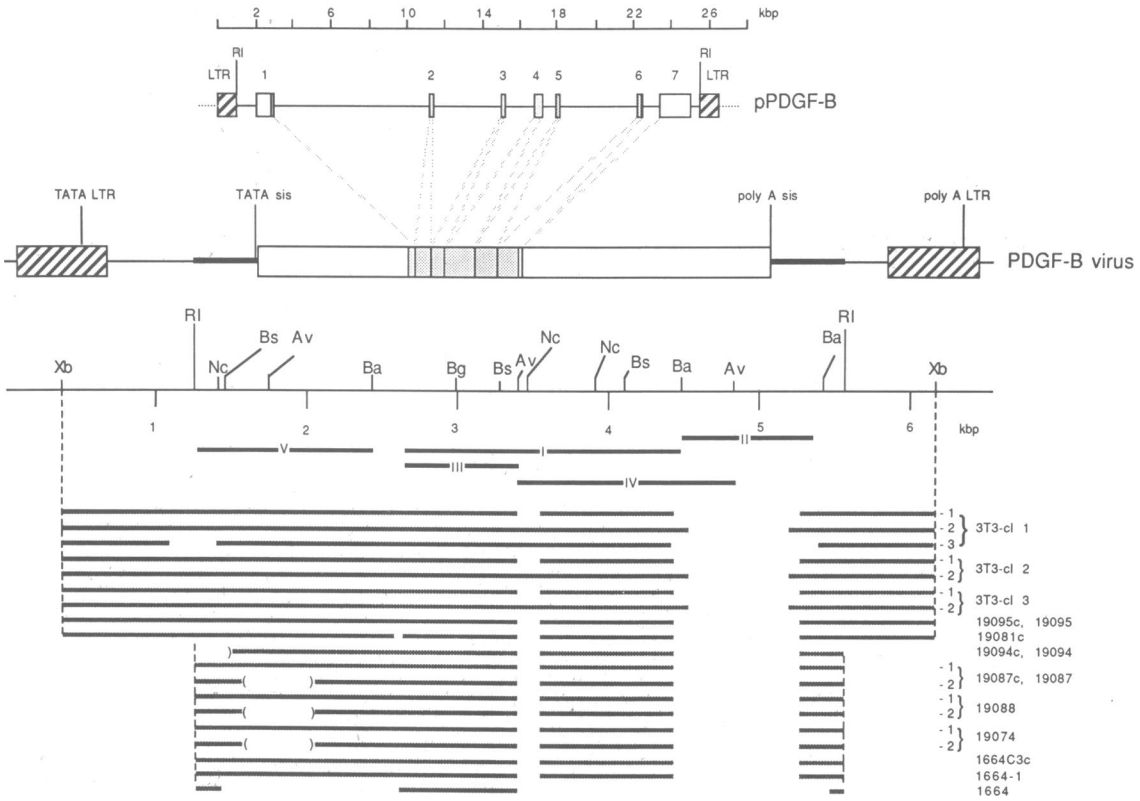

FIG. 4. Deletions within the PDGF-B virus. Mapping experiments with RNase protection assays and Southern blots were used to characterize the structure of PDGF-B viral RNAs and DNAs. Genomic PDGF-B sequences located between the *Eco*RI sites (RI) of pPDGF-B contain seven exons (boxed) with coding (stippled) and noncoding (open) sequences. Vector long terminal repeat (LTR) sequences are indicated by hatched boxes. The structure of a PDGF-B virus that would result from a faithful viral rescue of pPDGF-B-transfected NIH 3T3 cells is shown below the map of pPDGF-B. TATA signal sequences within the vector (TATA LTR) and the PDGF-B gene (TATA sis) as well as the respective polyadenylylation sites (poly A LTR/poly A sis) are indicated. Below the restriction map the location and sizes of probes I–V (heavy lines) are indicated. They were derived from PDGF-B cDNA sequences and were used to map PDGF-B proviruses present in fibrosarcomas and clonal NIH 3T3 transformants (3T3-cl1–3). Maps were established for the region between either the *Xba* I (Xb) or *Eco*RI sites. Stippled horizontal bars indicate where those maps were identical to the restriction map of an undeleted PDGF-B virus. Gaps represent sequences that were deleted during virus rescue or during propagation *in vitro* or *in vivo*. If the exact location of the deletions could not be determined, the gaps are flanked by parentheses. If a cell line or tumor contained more than one type of provirus, the different types were numbered 1–3. For restriction site abbreviations, see Fig. 2 legend. kbp, Kilobase pairs.

the structure of proviruses present within the fibrosarcomas, we employed a variety of PDGF-B cDNA and RNA probes in mapping proviral DNAs and RNAs in seven fibrosarcomas, five fibrosarcoma cell lines, and three *in vitro* transformed NIH 3T3 cell clones. As summarized in Fig. 4, all PDGF-B proviral variants had suffered various deletions at the 3′ end of the PDGF-B insert. These deletions consistently eliminated the PDGF-B polyadenylylation signal. In addition, all proviruses in the various fibrosarcomas and fibrosarcoma cell lines had an identical 149-bp deletion just downstream of the PDGF-B coding region. This RNA species, however, constituted <1% of PDGF-B-derived transcripts in pPDGF-B-transfected NIH 3T3 cells (Fig. 2). In NIH 3T3 cells transformed by the PDGF-B virus, proviral copies with and without the deletion could be detected (Fig. 4). These results indicated that while the viral RNA with the deletion was only a very minor component in the original transfected cell line, it was selected upon virus passage and transformation of new cells in culture and in tumors generated *in vivo*.

Retrovirus Generated from the Human PDGF-B Gene Mimics SSV in an Alternative Splice Pattern. To unambiguously localize the deletion, we sequenced the PDGF-B RNAs encoded by pPDGF-B and the PDGF-B proviral variants around the endpoints of the 149-bp deletion. The sequence of pPDGF-B RNA isolated from transfected NIH 3T3 cells could be read unambiguously and was identical to the published PDGF-B cDNA sequence (17). The viral RNAs isolated from the mouse fibrosarcomas, however, had deleted 149 nucleotides of 3′ noncoding sequence (between positions 1776 and 1926 of ref. 17). As shown in Fig. 5, this deletion was identical to the location of a gap that has to be introduced into the v-*sis* sequence when it is aligned with the PDGF-B cDNA sequence. Another splice acceptor site, located 149 bp further downstream of the equivalent site for exon 7 in the human PDGF-B gene, must have been used in the generation of SSV. Thus, the PDGF-B virus in the mouse fibrosarcomas precisely mimicked the alternative or aberrant splice pattern selected for in the generation of SSV.

DISCUSSION

In the present study, we tested the effects of high levels of expression of the normal human PDGF-B chain *in vivo*. Overexpression of this growth factor in cells possessing the cognate receptor resulted in tumor formation. Such tumors were invasive, could be propagated in athymic mice, and were histologically classified as fibrosarcomas independent of the site of inoculation. In their morphology, these tumors were similar to the spontaneous fibrosarcoma of the woolly monkey from which SSV was isolated (24).

While PDGF-B overexpression can induce malignant transformation of a continuous fibroblast line in culture (4), efforts to transform and immortalize diploid fibroblasts in response to either PDGF-B or SSV have been unsuccessful. There have been reports of focus formation (10, 25, 26), but

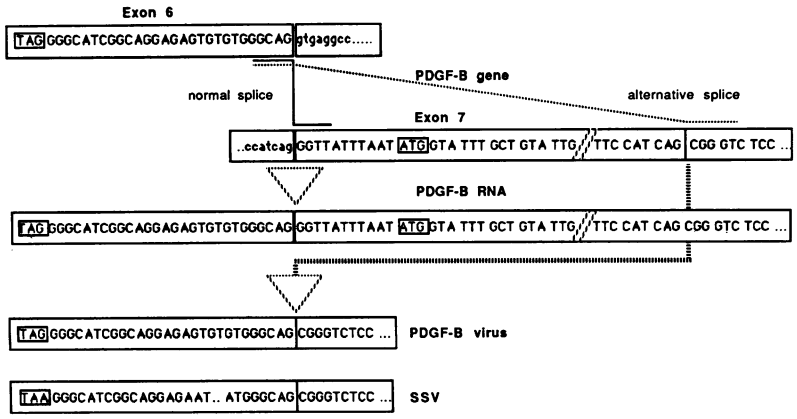

FIG. 5. PDGF-B virus mimics v-*sis* in an alternative splice pattern. RNAs were isolated from pPDGF-B-transfected cells and from fibrosarcomas 19074 and 19095c and sequenced around the exon 6/7 junction. Sequences in the pPDGF-B-transfected NIH 3T3 cells, which were used to rescue PDGF-B virus, were correctly spliced and identical to PDGF-B RNA (normal splice). PDGF-B virus-encoded RNAs in the fibrosarcomas (PDGF-B virus) were missing 149 nucleotides at the 6/7 junction. The v-*sis* sequence (SSV) aligns completely with the variant PGDF-B virus sequence at this alternative 6/7 junction. The termination codon for the first open reading frame, encoding the human PDGF-B chain or $p28^{v\text{-}sis}$ (SSV), and the initiation codon for a potential second open reading frame (107 amino acids) in PDGF-B RNA are indicated. Only part of this frame is shown (interrupted by broken lines). Sequences are shown as DNA, 5′ → 3′.

such growth-altered cells could not be established as permanent transformed cell lines. Yet, *in vivo*, the PDGF-B virus induced tumors that appeared to exhibit the fully malignant phenotype. Our analysis of proviral integration patterns in tumors and cell lines derived from such tumors indicated that superimposed upon polyclonal cell proliferation induced in response to PDGF-B virus expression in initially infected and virus-recruited cells, minor and major clonal subpopulations emerged. The latter exhibited all of the properties of fully neoplastic cells capable of rapid tumor formation upon transplantation. Thus, *in vivo* overexpression of this growth factor appeared capable of generating a sufficiently large target cell population to allow for selection of a fully neoplastic clone.

The concept (e.g., ref. 27) that protooncogenes are latent cellular oncogenes has been challenged on the basis of structural and functional differences between retroviral oncogenes and their cellular homologues (28). Despite the intact nature of the growth factor coding sequence itself, we were unable to recover PDGF-B virus containing the complete 3′ genomic PDGF-B region. The different deletions within the 3′ noncoding region that occurred during virus rescue and replication can in part be explained by the loss of the polyadenylylation signal sequence, which has been shown to interfere with retrovirus replication (29, 30).

We also mapped a 3′ deletion that occurred in all proviruses from fibrosarcomas, which indicated that the PDGF-B retrovirus was selected for an alternative or aberrant PDGF-B splice product. The histories of SSV and our PDGF-B virus are distinct. The human PDGF-B virus was created *in vitro*, whereas SSV arose by an undefined recombinational process involving the simian PDGF-B gene and its helper virus, SSAV. Nonetheless, when compared to the normal human PDGF-B transcript, both viral RNAs showed a deletion of 149 nucleotides within exon 7. This deletion destroys a second open reading frame with a translational initiation site (Fig. 5) that conforms to the consensus sequence suggested by Kozak (31). The second open reading frame could encode a protein of 107 amino acids. Whether the PDGF-B transcript is a polycistronic mRNA and the predicted product of the second open reading frame is expressed normally *in vivo* is not known. Previous studies have shown that the expression of the complete PDGF-B sequence, including this second open reading frame, under the control of a retroviral promoter in NIH 3T3 cells leads to the transformed phenotype (4). Thus, if this sequence were detrimental for transforming activity, it would have to be specific to malignant transformation of diploid cells. The presence of this sequence, in any case, must be detrimental for optimal growth of infected cells and/or for virus replication.

We thank Claire Y. Pennington for excellent technical assistance. We are grateful to Keith C. Robbins for his advice in the immunoprecipitation experiments. M.P. was supported by the Deutsche Forschungsgemeinschaft.

1. Doolittle, R. F., Hunkapiller, M. W., Hood, L. E., Devare, S. G., Robbins, K. C., Aaronson, S. A. & Antoniades, H. N. (1983) *Science* **221**, 275–277.
2. Waterfield, M. D., Scrace, G. T., Whittle, N., Stroobant, P., Johnsson, A., Wasteson, A., Westermark, B., Heldin, C. H., Huang, J. S. & Deuel, T. F. (1983) *Nature (London)* **304**, 35–39.
3. Chiu, I.-M., Reddy, E. P., Givol, D., Robbins, K. C., Tronick, S. R. & Aaronson, S. A. (1984) *Cell* **37**, 123–129.
4. Gazit, A., Igarashi, H., Chiu, I.-M., Srinivasan, A., Yaniv, A., Tronick, S. R., Robbins, K. C. & Aaronson, S. A. (1984) *Cell* **39**, 89–97.
5. Eva, A., Robbins, K. C., Andersen, P. R., Srinivasan, A., Tronick, S. R., Reddy, E. P., Ellmore, N. W., Galen, A. T., Lautenberger, J. A., Papas, T. S., Westin, E. H., Wong-Staal, F., Gallo, R. C. & Aaronson, S. A. (1982) *Nature (London)* **295**, 116–119.
6. Igarashi, H., Rao, C. D., Siroff, M., Leal, F., Robbins, K. C. & Aaronson, S. A. (1987) *Oncogene* **1**, 79–85.
7. Weiss, R., Teich, N., Varmus, H. & Coffin, J., eds. (1985) *RNA Tumor Viruses* (Cold Spring Harbor Lab., Cold Spring Harbor, NY).
8. Stewart, T. A., Pattengale, P. K. & Leder, P. (1984) *Cell* **38**, 627–637.
9. Jainchill, J. L., Aaronson, S. A. & Todaro, G. J. (1969) *J. Virol.* **4**, 549–553.
10. Wolfe, L. G., Deinhardt, F., Theilen, G. H., Rubin, H., Kawakami, T. & Bustad, L. K. (1971) *J. Natl. Cancer Inst.* **47**, 1115–1120.
11. Gardner, M. B., Officer, J. E., Rongey, R. W., Charman, H. P., Hartley, J. W., Estes, J. D. & Huebner, R. J. (1973) *Bibl. Haematol. (Basel)* **39**, 335–344.
12. Wigler, M., Silverstein, S., Lee, L.-S., Pellicer, A., Cheng, Y.-C. & Axel, R. (1977) *Cell* **11**, 223–232.
13. Southern, P. J. & Berg, P. (1982) *J. Mol. Appl. Genet.* **1**, 327–341.
14. Maniatis, T., Fritsch, E. F. & Sambrook, J. (1982) *Molecular Cloning: A Laboratory Manual* (Cold Spring Harbor Lab., Cold Spring Harbor, NY).
15. Srinivasan, A., Dunn, C. Y., Yuasa, Y., Devare, S. G., Reddy, E. P. & Aaronson, S. A. (1982) *Proc. Natl. Acad. Sci. USA* **79**, 5508–5512.
16. Reddy, E. P., Smith, M. J. & Srinivasan, A. (1983) *Proc. Natl. Acad. Sci. USA* **80**, 3623–3627.
17. Rao, C. D., Igarashi, H., Chiu, I.-M., Robbins, K. C. & Aaronson, S. A. (1986) *Proc. Natl. Acad. Sci. USA* **83**, 2392–2396.
18. Rao, C. D., Igarashi, H., Pech, M. W., Robbins, K. C. & Aaronson, S. A. (1986) *Cold Spring Harbor Symp. Quant. Biol.* **51**, 959–966.
19. Rao, C. D., Pech, M., Robbins, K. C. & Aaronson, S. A. (1988) *Mol. Cell. Biol.* **8**, 284–292.
20. Parnes, J. R. & Seidman, J. G. (1982) *Cell* **29**, 661–664.
21. Ponte, P., Ng, S.-Y., Engel, J., Gunning, P. & Kedes, L. (1984) *Nucleic Acids Res.* **3**, 1687–1696.
22. Geliebter, J., Zeff, R. A., Melvold, R. W. & Nathenson, S. G. (1986) *Proc. Natl. Acad. Sci. USA* **83**, 3371–3375.
23. Melton, D. A., Krieg, P. A., Rebagliati, M. R., Maniatis, T., Zinn, K. & Green, M. R. (1984) *Nucleic Acids Res.* **12**, 7035–7056.
24. Theilen, G. H., Gould, D., Fowler, M. & Dungworth, D. L. (1971) *J. Natl. Cancer Inst.* **47**, 881–889.
25. Aaronson, S. A. (1973) *Virology* **52**, 3069–3072.
26. Johnsson, A., Betsholtz, C., Heldin, C. H. & Westermark, B. (1986) *EMBO J.* **5**, 1535–1541.
27. Bishop, J. M. (1987) *Science* **235**, 305–311.
28. Duesberg, P. H. (1987) *Proc. Natl. Acad. Sci. USA* **84**, 2117–2124.
29. Temin, H. (1982) *Cell* **28**, 3–5.
30. Gazit, A., Pierce, J. H., Kraus, M. H., Di Fiore, P. P., Pennington, C. Y. & Aaronson, S. A. (1986) *J. Virol.* **60**, 19–28.
31. Kozak, M. (1986) *Cell* **44**, 283–292.